



Supplementary Materials for

TTC5 Mediates Autoregulation of Tubulin via mRNA Degradation

Zhewang Lin, Ivana Gasic, Viswanathan Chandrasekaran, Niklas Peters, Sichen Shao,
Timothy J. Mitchison, and Ramanujan S. Hegde

correspondence to: rhegde@mrc-lmb.cam.ac.uk

This PDF file includes:

Materials and Methods
Figs. S1 to S14
Table S1

Materials and Methods

Plasmids and reagents

Tubulin constructs (human TUBB and TUBA1B) for in vitro translation in reticulocyte lysate (RRL) were cloned into pCDNA3.1. Constructs used for the expression and purification of WT or mutants 6XHis-StrepII-TTC5 human recombinant proteins were in the pET28a vector. Mutant *E.coli* tyrosyl-tRNA synthetase for incorporation of Bpa (31) was expressed and purified from pET21 vector. *Bacillus stearothermophilus* suppressor tRNA^{Tyr} sequence (32) carrying 5' T7 promoter sequence and a 3' BSTN1 restriction site was cloned into pRSET. For generation of stable cell lines, human TTC5 WT or mutants were sub-cloned into the pcDNA 5/FRT/TO vector. CRISPR Cas9 mediated TTC5 knockout used the following guide RNAs in the pX459 plasmid:

Exon 2 guide: (5'-TCATACTTTTTAGGAACTCG-3')

Exon 3 guide: (5'- TCAGCCTTAGGGCTATAGTC -3')

Exon 4 guide: (5'- GCTGACGAAGCACCATTGAC -3')

Cell Cultures

Flp-In TRex 293 cells (Invitrogen) were maintained in DMEM supplemented with 10% fetal calf serum and 2 mM L-glutamine. Flp-In TRex HeLa cells (from Brian Raught, University of Toronto) were maintained in DMEM supplemented with 10% fetal calf serum. CRISPR-Cas9 mediated gene disruption was performed in the Flp-In TRex 293 and HeLa cells as described (33). Briefly, cells were transiently transfected with the pX459 plasmid encoding the gRNAs targeting TTC5. 24 hours after transfection, 2 µg/ml puromycin was added for selection. 3 days after transfection, cells were trypsinized and re-plated in 96-well plates at a density of 0.5 cells per well to obtain single cell clones. Successful knockout clones were verified by anti-TTC5 western blot (TTC5 Polyclonal Antibody, Epigentek A66330 and Novus Biologicals NBP1-76636) and genotyping via PCR amplification of the modified region (see fig. S15 for an example). TTC5 rescue cell lines with stable expression of N-terminal FLAG-tagged WT or mutant TTC5 were generated from the TTC5-knockout cells using the Flp-In system (Invitrogen) according to manufacturer's protocol. Expression of transgene was induced with doxycycline (1 µg/mL) for 24-48h. Colchicine (10 µM), nocodazole (10 µM), and combretastatin A4 (1 µM) treatments were performed in standard media for the indicated time.

Live cell imaging and data analysis

Flp-In TRex HeLa of the genotypes indicated in the figure legends were plated in 8-well Lab Tek II Chamber 1.5 German coverglass dishes (Thermo Fisher, 155409) in regular growth medium, and incubated for 6 hours. Medium was then changed to DMEM with HEPES and without phenol-red (Thermo Fisher, 21063045) supplemented with 10% fetal calf serum, 10 ng/ml doxycycline and 200 nM SiR-DNA (Cytoskeleton, CY-SC007). Cells were incubated for 24 hours prior to imaging. Time lapse images were acquired using widefield inverted Nikon Ti fluorescence microscope (Nikon), equipped with Hamamatsu ORCA-ER cooled CCD camera (Hamamatsu), Proscan III motorized stage and shutters (Prior Scientific), SOLA light engine for fluorescence illumination (Lumencor), perfect focus system, and an incubation chamber with 37 C and 5% CO₂

cage (OkoLab). Three-dimensional Images at multiple stage positions were acquired in steps of 2 μm , every 7 minutes for 10 hours using MetaMorph (Molecular Devices) and 20x PlanApo objective (NA 0.75, Nikon). Single images were reconstructed into 3D movies using Fiji (ImageJ). Maximum intensity projections of representative examples of mitoses were prepared in Fiji and exported either as movies or still images. Analysis of mitotic cells was performed using 3D reconstructions in Fiji. The parameters scored (based on SiR-DNA signal) were time from nuclear envelope breakdown (NEB) to telophase (two-cell stage), occurrence of unaligned chromosomes in metaphase, and chromosome segregation errors in anaphase. Data analyses were documented using Excel and processed and plotted using R. Statistical analyses were performed in R and Excel.

Recombinant protein and tRNA purification

WT and mutant 6XHis-StrepII tagged TTC5 were purified from *E. coli* (BL21) cells. Briefly, cells were transformed with the pET28a plasmid encoding the WT or mutant TTC5 and grown at 37 °C in LB containing 50 $\mu\text{g}/\text{mL}$ kanamycin. Induction was with 0.2 mM IPTG at an A600 of 0.6 at 16 °C overnight. For Bpa incorporation at position 194 in TTC5 protein, the cells were co-transformed with the pET28a plasmid encoding the amber mutant TTC5 and the pEVOL-pBpF plasmid [addgene #31190; (34)]. Cells were grown at 37 °C in LB containing 50 $\mu\text{g}/\text{mL}$ kanamycin and 25 $\mu\text{g}/\text{mL}$ chloramphenicol and induced with 0.2% L-arabinose at an A600 of 0.3 for 30 min followed by a second induction with 0.2 mM IPTG at an A600 of \sim 0.6 at 16 °C overnight. Bacterial lysate was prepared by sonication in 30 mL cold lysis buffer (500 mM NaCl, 20 mM imidazole, 1 mM phenylmethylsulfonyl fluoride, 1 mM TCEP and 50 mM HEPES, pH 7.4) per L of cells. Clarified bacterial lysates from a 1 L culture were bound to 1 mL column of Ni-NTA (Qiagen) by gravity flow. Columns were washed with \sim 10 column volumes of lysis buffer and eluted with 250 mM imidazole in lysis buffer. The eluate was then bound to a 200 μL column of Streptactin Sepharose® High Performance (GE Healthcare, 28-9355-99). After extensive washing with 500 mM NaCl, 1 mM TECP and 20 mM Hepes, pH 7.4, the bound TTC5 protein was eluted with 500 μL washing buffer containing 25 mM biotin and dialyzed twice against dialysis buffer (500 mM NaCl, 1 mM TECP and 20 mM Hepes, pH 7.4). *E. coli* Bpa tyrosyl-tRNA synthetase was purified via the C-terminal His tag on a 5 mL HiTrap Ni-NTA column (GE), desalted by a gel filtration column on FPLC and concentrated by Amicon Ultra centrifugal filter (Millipore, Z717185-8EA). *B. stearothermophilus* tRNA^{Tyr}, was synthesized by in vitro transcription. The pRSET-based construct was digested with BSTN1, yielding a DNA fragment containing the exact tRNA^{Tyr} sequence under a T7 promoter. 5 mL transcription reaction was carried out with 1.2 mg DNA template, 1 mM spermidine, 5 mM DTT, 0.1% Triton, 5 mM NTPs, 25 μM MgCl₂, 20 $\mu\text{g}/\text{mL}$ *E. coli* pyrophosphatase, 20 $\mu\text{g}/\text{mL}$ T7 polymerase and 125 U Recombinant RNasin (Promega) for 4 hours at 37 °C. The reaction product was digested with Turbo DNase (Ambion) and extracted by acid phenol chloroform extraction to yield purified tRNA.

Western blot analysis

Samples were analyzed using 12% Tris-Tricine based gels, and transferred to 0.2 mm nitrocellulose membrane (Biorad). Primary antibody incubations were either for 1h at room temperature or 4 °C overnight. Detection used HRP-conjugated secondary

antibodies and SuperSignal West Pico Chemiluminescent substrate (Thermo Fisher), or DyLight conjugated antibodies (Thermo Fisher) and Odyssey Infra-Red Imaging System (LI-COR). Expression of N-FLAG WT or mutant TTC5 in rescue cell lines was detected by anti-FLAG M2-HRP (Sigma A8592), or monoclonal anti-FLAG M2 (Sigma, F3165). RPL8 protein was detected by anti-RPL8 antibody (abcam, ab155136), and tubulin proteins by anti- α -tubulin antibody (Sigma, T6199) or anti- β -tubulin antibody (Cell Signaling Technologies, 2128).

In vitro transcription and translation

All in vitro transcription of tubulin constructs utilized PCR product as template. The 5' primer contains the SP6 promoter sequence and anneals to the CMV promoter of pCDNA3.1. The 3' primers anneal at codon 54-60 or 84-90 of nascent tubulin and contain extra sequence encoding MKLV to generate 64-mer or 94-mer constructs respectively. Transcription reactions were carried out with SP6 polymerase for 1 hour at 37 °C. Transcription reactions were directly used for in vitro translation in a homemade rabbit reticulocyte lysate (RRL)-based translation system as previously described (35, 36). For incorporation of Bpa by amber suppression, 5 μ M B. Stearothermophilus tRNA^{Tyr}, 0.25 μ M Bpa tyrosyl-tRNA synthetase, and 0.1 mM Bpa were included in the translation reaction. Where indicated in the figure legends, WT or mutant 6XHis-strepII-tagged TTC5s were included in the translation reactions. Translation reactions were at 32 °C for 20 min unless stated otherwise. For analysis of total translation level of nascent chains, a 1 μ L aliquot of the translation reaction was mixed with protein sample buffer and analyzed by SDS-PAGE gel electrophoresis and autoradiography.

TTC5-RNC UV crosslinking analysis

Crosslinking was performed on isolated RNCs stalled after synthesis of a defined number of amino acids. Stalling was achieved by using a transcript truncated within the coding region at the desired codon (35, 36). When ribosomes reach the end of such a mRNA, they stall. To isolate the stalled RNCs, 50 μ L translation reactions were rapidly cooled on ice and layered on a 200 μ L sucrose cushion in physiological salt buffer (PSB: 50 mM Hepes, pH 7.4, 100 mM KAc, 2 mM MgCl₂). Centrifugation was in a TLA 120.1 rotor (Beckman) at 100,000 rpm for 1 hour at 4 °C. The ribosome pellets were resuspended in 20 μ L PSB on ice. The isolated RNCs were placed on ice ~10 cm away from a UVP B-100 series lamp (UVP LLC) for 10 minutes. For analysis of total crosslinking products, 2.5 μ L of the reactions were mixed directly with protein sample buffer for SDS-PAGE gel electrophoresis and analyzed by autoradiography. For immunoprecipitation of tubulin nascent chain and endogenous TTC5 crosslinking product, 20 μ L of the crosslinking reactions were adjusted to 1% SDS, denatured by heating at 95 °C for 1 min, diluted 10 fold with 180 μ L IP buffer (100 mM NaCl, 50 mM Hepes, pH 7.4, 1% Triton X-100) and incubated with 1 μ g of TTC5 antibody and 5 μ L of protein A agarose at 4 °C for 2 hours. Beads were washed three times with 400 μ L IP buffer and eluted with protein sample buffer for SDS-PAGE gel electrophoresis and autoradiography. For TTC5-RNC UV crosslinking in the presence of cytosolic lysates, isolated RNCs were pre-incubated with 2 mg/mL lysates for 5 min on ice before UV crosslinking. Note that cell lysates were prepared on ice. At this temperature, nearly all microtubules depolymerize during lysate preparation, and the minor population that does not is removed by centrifugation. Thus,

the cell lysates do not contain intact microtubules, and the soluble tubulin content of lysates prepared from untreated and colchicine/nocodazole treated cells are the same. For this reason, the inhibitor detected in Fig. 4B is not likely to be polymerized tubulin.

Quantitative mass spectrometry analysis of RNC associated proteins

Total ribosomes and associated proteins from translation reactions of WT or mutant nascent β -tubulin 64-mer were isolated by centrifugation as described above. The experiment was performed in duplicate. Quantitative mass spectrometry was performed by in-solution digestion of samples, followed by tandem mass tag labelling (Thermo Fisher Scientific cat. #90110). Protein samples in solution were reduced with 5 mM DTT at 56 °C for 30 min and alkylated with 10 mM iodoacetamide for 30 min in the dark at 22 °C. The alkylation reaction was quenched by the addition of DTT and the samples were digested with trypsin (Promega, 0.5 μ g) overnight at 37 °C. The peptide mixtures were then desalted using home-made C18 (3M Empore) stage tip filled with 0.5mg of poros R3 (Applied Biosystems) resin. Bound peptides were eluted sequentially with 30%, 50% and 80% acetonitrile in 0.1%TFA and lyophilized. Dried peptide mixtures from each condition were resuspended in 20 μ L of 7% acetonitrile, 200 mM triethyl ammonium bicarbonate. For TMT labelling, 0.8 mg of TMT reagents (Thermo Fisher Scientific) were reconstituted in 41 μ L anhydrous acetonitrile. 10 μ L of TMT was added to each peptide mixture and incubated for 1 hour at room temperature. The labelling reactions were terminated by incubation with 2.5 μ L 5% hydroxylamine for 15 min, and labelled samples were subsequently pooled. The acetonitrile was evaporated using a Speed Vac, desalted and then fractionated with home-made C18 (3M Empore) stage tip using 10 mM ammonium bicarbonate and acetonitrile gradients. Eluted fractions were partially dried down using a Speed Vac and subjected to LC-MSMS. Liquid chromatography was performed on a fully automated Ultimate 3000 RSLC nano System (Thermo Scientific) fitted with a 100 μ m \times 2 cm PepMap100 C18 nano trap column and a 75 μ m \times 25 cm reverse phase C18 nano column (Acclaim PepMap, Thermo Scientific). Samples were separated using a binary gradient consisting of buffer A (2% acetonitrile, 0.1% formic acid) and buffer B (80% acetonitrile, 0.1% formic acid). Peptides were eluted at 300 nL/min with an acetonitrile gradient. The HPLC system was coupled to a Q Exactive Plus hybrid quadrupole-Orbitrap mass spectrometer (Thermo Fisher Scientific) equipped with a nanospray ion source. The acquired MSMS raw files were processed using Proteome Discoverer (version 2.1, Thermo Scientific). MSMS spectra were searched against mammals, UniProt Fasta database using Mascot (version 2.4, Matrix Science) search engine.

Affinity purification of TTC5-RNC complex

For analytical experiments, 20 μ L translation reactions of nascent β -tubulin 64-mer containing 250 nM WT or mutant 6XHis-StrepII tagged TTC5s were carried out. The reactions were diluted 10 fold with 180 μ L PSB and incubated with 5 μ L streptactin sepharose at 4 °C for 2 hours. Beads were washed four times with 400 μ L PSB and eluted with 20 μ L 25 mM biotin in PSB at 4 °C for 30 min. Eluates were mixed with protein sample buffer for SDS-PAGE gel electrophoresis and analyzed with sypro ruby protein gel stain (Thermo Fisher Scientific cat. S12000). For preparative scale purification of the TTC5-RNC complex for cryo-EM analysis, a 2 mL translation reaction containing 250

nM WT 6XHis-StrepII tagged TTC5 and non-radioactive methionine (40 μ M) was incubated at 32 °C for 30 min. The reaction was cooled on ice and incubated with 20 μ L streptactin sepharose at 4 °C for 2 hours. Beads were washed four times with 400 μ L PSB and eluted with 40 μ L 25 mM biotin in PSB at 4 °C for 30 min.

Thermal shift assay

The binding of synthetic peptides to recombinant TTC5 proteins were analyzed by thermal melting temperature using the nano-Differential Scanning Fluorimetry (NanoDSF, 2bind). 4 μ M of WT or mutant TTC5 proteins were mixed with the indicated synthetic peptides (custom peptide synthesis by Genescript) in 100 mM HEPES pH 7.4, 250 mM NaCl. The capillaries were filled with 10 μ L samples and placed on the sample holder. A temperature gradient of 2 °C \cdot min⁻¹ from 25 to 95 °C was applied and the intrinsic protein fluorescence at 330 and 350 nm was recorded. The first derivative of the 350 nm and 330 nm fluorescence ratio was plotted. The maximum of the peak corresponds to the melting temperature of the protein (inflection point of the ratio curve).

RT-qPCR for mRNA

HEK293 cells were grown to 70-80% confluency in 35 mm dish and treated with DMSO (control), colchicine (10 μ M) or nocodazole (10 μ M) for 3 hours. Cells were harvested and total RNA isolated using the RNeasy mini kit (QIAGEN, 74104) as per the manufacturers protocol. On column DNase digestion was performed. 500 ng of total RNA was used to generate cDNA using the iScript cDNA synthesis kit (BioRad). Samples were then kept on ice while they were made up to a volume of 100 μ L with nuclease-free water. Small quantities of all samples were pooled and subsequently serially diluted to make standards. Samples were diluted ten-fold to ensure their values fell within the standard curve. RT-qPCR was carried out using a ViiA 7 Real-Time PCR System (Thermo Fisher Scientific) and KAPA SYBR Fast qPCR reagents (KAPA Biosystems) as per manufacturers instructions. The primer sequences used are listed below. All pairs of primers were annealed at 60 °C, and a melt curve performed. PCR products were verified by sequencing. Data was then analyzed using the Quantstudio Real-time PCR software v1.3. Values were normalized to the standard curve and against RPLP1 or GAPDH. Experiments include three biological replicates.

HeLa cells were grown to 70-80% confluency in 100 mm dishes and treated with DMSO (control) or combretastatin A4 (1 μ M) 4 hours. Cells were harvested and total RNA isolated using the PureLink RNA Mini Kit (Invitrogen, Thermo Fisher, 12183018A) as per the manufacturers protocol. On column DNase digestion was performed using PureLink DNase Set (Thermo Fisher, 12185010) as per manufacturer's instructions. 500 ng of total RNA was used to generate cDNA using the SuperScript IV (Invitrogen, 18091050) and random hexamer primers, and following manufacturer's protocol. Samples were serially diluted to make standards. RT-qPCR was carried out using 5 ng of cDNA and 2x PowerUp SYBR Green master mix (Thermo Fisher, A25776) on a BioRad thermocycler (BioRad), as per manufacturer's instructions. Previously described and validated primers were used (5). All pairs of primers were annealed at 60 °C, and a melt curves performed. Data analysis was performed using the ddCt method (37). All data were normalized to reference genes RPL19 or GAPDH, and to DMSO

treated controls. Experiments include three biological replicates. Processing, statistical analysis, and data plotting were performed in R.

RT-qPCR primers used in this study

Target gene	Description	Sequence
TUBA1B	mRNA Forward	5'-AATTCGCAAGCTGGCTGA-3'
	mRNA Reverse	5'-CGACAGATGTCATAGATGGCC-3'
	pre-mRNA Forward	5'-CACAGTCATTGGTGAGTTGAC-3'
	pre-mRNA Reverse	5'-GTGCTTACCAGCTTGCGAAT-3'
TUBA1A	mRNA Forward	5'-CCACAGTCATTGATGAAGTTTCG-3'
	mRNA Reverse	5'-GCTGTGGAAAACCAAGAAGC-3'
	pre-mRNA Forward	5'-GCAGCATTGTAGCAGGTGA-3'
	pre-mRNA Reverse	5'-GCATTGCCAATCTGGACAC-3'
TUBB	mRNA Forward	5'-GAAGCCACAGGTGGCAAATA-3'
	mRNA Reverse	5'-CGTACCACATCCAGGACAGA-3'
	pre-mRNA Forward	5'-CTGGACCGCATCTCTGTGTA-3'
	pre-mRNA Reverse	5'-GGTTCACGAAAGGGACAAAA-3'
GAPDH	mRNA Forward	5'-AGCTCATTCCTGGTATGACA-3'
	mRNA Reverse	5'-AGGGGAGATTCAGTGTGGTG-3'
RPLP1	mRNA Forward	5'-CTCACTTCATCCGGCGACTAG-3'
	mRNA Reverse	5'-GCAGAATGAGGGCCGAGTAG-3'
RPL19	mRNA Forward	5'-ATCGCCACATGTATCACAGC-3'
	mRNA Reverse	5'-TTGGTCTCTCCTCCTTGGAT-3'

Recombinant TTC5 pulldown assays of cell lysates

TTC5-knockout cells were grown to 70-80% confluency in 145 mm dish and treated with DMSO control, colchicine (10 μ M) or nocodazole (10 μ M) for the times indicated in the figure legends. For preparation of cytosolic cell lysates, cells were pelleted by centrifugation at 500g for 5 min and lysed with lysis buffer [100 mM KAc, 5 mM MgAc₂, 1 mM DTT, 100 μ g/mL digitonin, 1X EDTA-free protease inhibitor cocktail (Roche) and 50 mM HEPES, pH 7.4] for 10 min on ice. Lysates were cleared by centrifugation at 20,000 g for 5 min at 4 °C. Lysate concentrations were determined by Pierce BCA assay kit (Thermo Fisher). Note that on ice, nearly all microtubules depolymerize. Thus, the cell lysates do not contain microtubules, and the soluble tubulin content of lysates prepared from untreated and colchicine/nocodazole treated cells are the same. An aliquot of the lysates was used for total cytosolic RNA extraction and analyzed for tubulin mRNA content by RT-qPCR as described above. Another aliquot of each lysates was incubated with 500 nM recombinant TTC5 for 2 min on ice and incubated with 10 μ L streptactin sepharose for 2 hours at 4 °C to recover TTC5 and all bound components. Control samples omitted recombinant TTC5. Beads were washed three times with 400 μ L PSB and eluted with 50 μ L 25 mM biotin in PSB at 4 °C for 30 min. The eluted products were used to isolate RNA using the RNeasy mini kit and used to generate cDNA using the iScript cDNA synthesis kit. Tubulin mRNAs in the elution were analyzed via RT-qPCR as described above.

Pulse labelling of protein synthesis

Cells were grown to 70-80% confluency in 35mm dish prior to labelling. Cells were washed two times with 2mL warm 1XPBS and starved for 30 min at 37 °C in media

lacking methionine. Labelling was initiated by addition of ^{35}S -methionine to a final concentration of 100 μCi per ml and incubated at 37 °C for 30 min. After the labeling period, cells were pelleted by centrifugation at 500 g for 2 min at 4 °C and lysed with 200 μL lysis buffer [100 mM KAc, 5 mM MgAc_2 , 1 mM DTT, 100 $\mu\text{g}/\text{mL}$ digitonin, 1X EDTA-free protease inhibitor cocktail (Roche) and 50 mM HEPES, pH 7.4] for 10 min on ice. 3 μL of cleared lysate was mixed with protein sample buffer for SDS-PAGE to detect total translation product via autoradiography. For immunoprecipitation of α - and β -tubulin, 50 μL of the lysate was denatured by heating at 95 °C for 1 min after addition of 1% SDS, diluted 10 fold with 450 μL IP buffer (100 mM NaCl, 50 mM Hepes, pH 7.4, 1% Triton X-100) and incubated with 1 μg of anti- α -tubulin (Sigma T6199) or anti- β -tubulin (Sigma T7816) antibody and 5 μL of protein G agarose at 4 °C for 2 hours. Beads were washed four times with 400 μL IP buffer and eluted with protein sample buffer for SDS-PAGE gel electrophoresis and autoradiography.

Cryo-EM grid preparation and data collection

Affinity-purified TTC5-RNCs were adjusted to ~ 100 nM (A_{260} of 6) with PSB and vitrified on UltrAuFoil R2/2 300-mesh grids (Quantifoil) coated with graphene oxide (Sigma). Briefly, grids were rinsed in deionized water, air-dried and glow-discharged for 4 min using an Edwards S150B sputter coater at 0.1 torr and 30 mA. 3 μL of 0.2 mg/mL graphene oxide suspension (Sigma Cat #763705-100ML) was overlaid for 1 min, blotted on filter paper and washed three times in deionised water (twice from the sample side, once from the back) and air-dried. 3 μL of sample was pipetted onto graphene oxide-coated grids, incubated for 30 s, blotted using Whatman filter paper grade 597 for 4 s with a blot force of -15 and plunge-frozen in liquid ethane at 92 K using a Vitrobot Mark IV (Thermo Fisher Scientific). Grids were stored in liquid nitrogen until use. The dataset was recorded on a FEI Falcon III camera in integrated mode on a Titan Krios G3 microscope using EPU software. The dataset contained 2805 movies (39 frames; a dose of 1.25 e- frame-1 \AA^{-2} ; 1s exposure; 59,000X magnification), resulting in a pixel size of 1.339 \AA (refer to Table S1 for data statistics).

Cryo-EM data processing

All data processing steps were performed in RELION-3 (38). Movies were aligned as 9 x 9 patches using MotionCor2 (39) with dose-weighting. Contrast transfer function (CTF) was estimated using CTFFIND-4.1 (40) and 2669 micrographs with good CTF (and corresponding to a CTF figure of merit > 0.3 and maximum resolution better than 5 \AA) were selected for further processing. 234,788 particles were picked using a 20 \AA lowpass-filtered 80S ribosome 3D reference and extracted in a 400-pixel box, which was then downsampled into a 128 pixel box (4.16 $\text{\AA}/\text{pixel}$). Following visual confirmation of the high quality of data, 2D classification was bypassed and initial three-dimensional refinement was carried out using a 70 \AA lowpass-filtered map of a rabbit ribosome as reference to yield a starting ribosome map at Nyquist resolution (8.44 \AA) with an estimated angular accuracy of 0.75°. Clear density was visible near the nascent chain tunnel exit for factors later identified as TTC5 and nascent chain-associated complex (NAC).

To enrich for populations containing these factors, focused classification with partial signal subtraction (FCwSS) was performed on the data with soft masks to protect the

factors while subtracting signal corresponding to the rest of the ribosome. 3D-classification without alignment of the subtracted particles into 5 classes yielded a class of active 80S ribosomes with a P-site tRNA and strong density for TTC5 and NAC (23%, 54,865 particles) and this subset was refined to an angular accuracy of 0.67°, re-extracted in a 400-pixel box (1.339 Å/pixel) and re-refined to 0.43° angular accuracy and 3.72 Å resolution. A second class (64%, 149,936 particles) containing NAC density but not TTC5 density was also obtained and presumably represents particles that had lost TTC5 during vitrification. This class was refined to an angular accuracy of 0.7°, re-extracted in a 400-pixel box (1.339 Å/pixel) and re-refined to 0.4° angular accuracy and 3.3 Å resolution. Particles in the TTC5-containing class were next subjected to Bayesian polishing and 3D refinement, which improved the resolution to 3.57 Å.

Because density for the 40S was smeared due to a mixture of subunit rotation states, we subtracted the 40S and focused on the 60S-TTC5 regions of the map. This step resulted in an improved resolution of 3.3 Å. A second round of FCwSS on TTC5 density was performed on the polished, 40S-subtracted particles (which eliminated ~ 3% of particles) and CTF refinement was performed to improve estimations of beamtilt, per-particle defocus and per-particle astigmatism. These steps resulted in an improved angular accuracy of 0.34° and a final, gold-standard resolution of 3.1 Å.

Local resolution and map quality of TTC5 and the bound tubulin nascent chain residues suffered from some degree of flexibility of TTC5 relative to the ribosome. To improve the alignment, we therefore also performed focussed 3D refinement of TTC5 density with signal from the ribosome subtracted. Briefly, TTC5 density was masked, centered and re-extracted in a 200-pixel box (1.339 Å/pix) and signal from the 60S was subtracted. The particles were then refined with a local angular search of 0.9° to minimize overfitting and prevent diverging angular assignments. The resulting map (fig. S5A) was at a modest resolution of 6.8 Å but had clear density in the nascent chain binding pocket.

Model building, refinement and validation

To build a model for the TTC5-bound ribosome, rRNA, P-site tRNA and protein chains from the 60S of PDB 5LZS (41) were first docked into the sharpened, modulation transfer function (MTF)-corrected density. Clear, unambiguous density was visible for the β -tubulin nascent chain inside the ribosome exit tunnel (residues 37-64) and this region was modelled *de novo*. The bond between the 3' O of A76 of the P-site tRNA and the carbonyl C of valine 64 was added as a custom bond geometric restraint via an additional parameter input file during refinement in phenix.real_space_refine. Density for the TTC5-bound residues 1-8 of nascent β -tubulin was observed at a lower resolution owing to flexibility of TTC5 relative to the 60S. These residues were therefore modelled conservatively as C β stubs and held in place during real-space refinement via an additional reference model input file. A TTC5 homology model based on the crystal structure of mouse TTC5 [PDB 4ABN; (42)] was derived using SWISS-MODEL (43), and adjusted to fit the density using ProSMART restraints in Coot (44, 45). The NAC model was derived from PDB 3MCB (46). A putative N-terminal extension of NAC α that is not seen in previous NAC structures was observed to insert between ribosomal proteins eL19 and eL22 and was modeled as poly-Ala. The overall model was adjusted manually in Coot to conform with the density using suitably blurred maps (with B-factors between

0 and 100), saved in mmCIF/PDBx format and real space-refined using phenix.real_space_refine. The 40S was simply modeled in the canonical state via structural superimposition of PDB 5LZS. Model statistics (Table S1) were generated automatically using Molprobit via the Phenix GUI (47). All reported resolutions are based on the Fourier shell correlation (FSC) 0.143 criterion (48).

Molecular graphics

Structural figures were generated using Pymol (Schrödinger, LLC) and UCSF Chimera (49). The FSC curve was generated in Microsoft Excel and annotated in Adobe Illustrator.

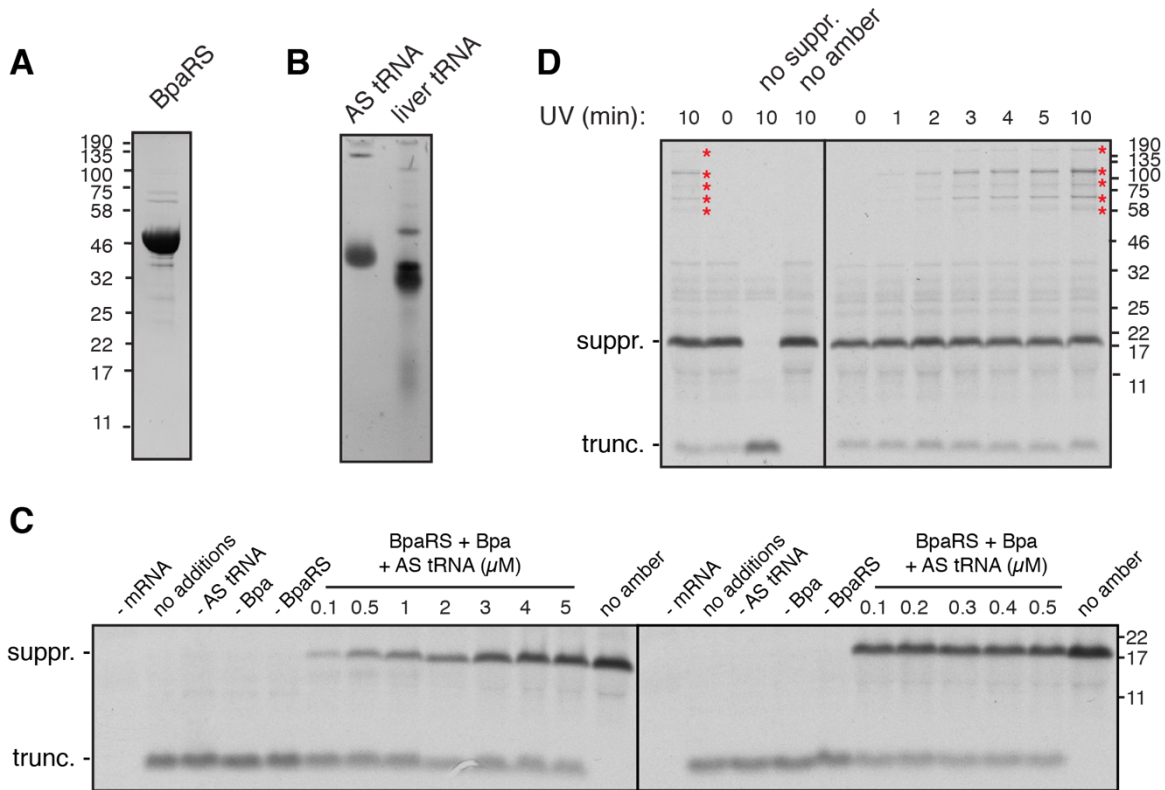


Fig. S1 - Characterization of amber-suppressor mediated photo-crosslinking in vitro

(A) Coomassie stained gel of purified tRNA synthetase (BpaRS) for charging of benzoyl-phenylalanine (Bpa). (B) Stained acrylamide gel of in vitro transcribed and purified amber-suppressor tRNA (AS tRNA) compared to a comparable amount of total porcine liver tRNA. (C) In vitro translation in rabbit reticulocyte of a 35 S-labelled 143 amino acid protein (encoding the N-terminal fragment of the β 1-adrenergic receptor) containing an amber codon at position 52 (within the first transmembrane domain). The first lane of each panel lacks mRNA, and the last lane of each panel contains a version of the construct lacking the amber codon. Other lanes contained various combinations of Bpa, BpaRS, and AS tRNA as indicated. The positions of the truncated product (i.e., terminated at the amber codon) and the amber-suppressed product are indicated. (D) Translation reactions of the amber containing protein from panel C were performed with Bpa, BpaRS, and AS tRNA under optimized conditions as identified in panel C. Lane 3 lacks the components for amber suppression, and lane 4 contains mRNA for a matched protein lacking an amber codon. After the translation reaction, the samples were irradiated with UV light for the indicated times. The positions of suppression-dependent and UV-dependent crosslinking partners are indicated by red asterisks. These are cytosolic chaperones that interact with the transmembrane domain of the translation product.

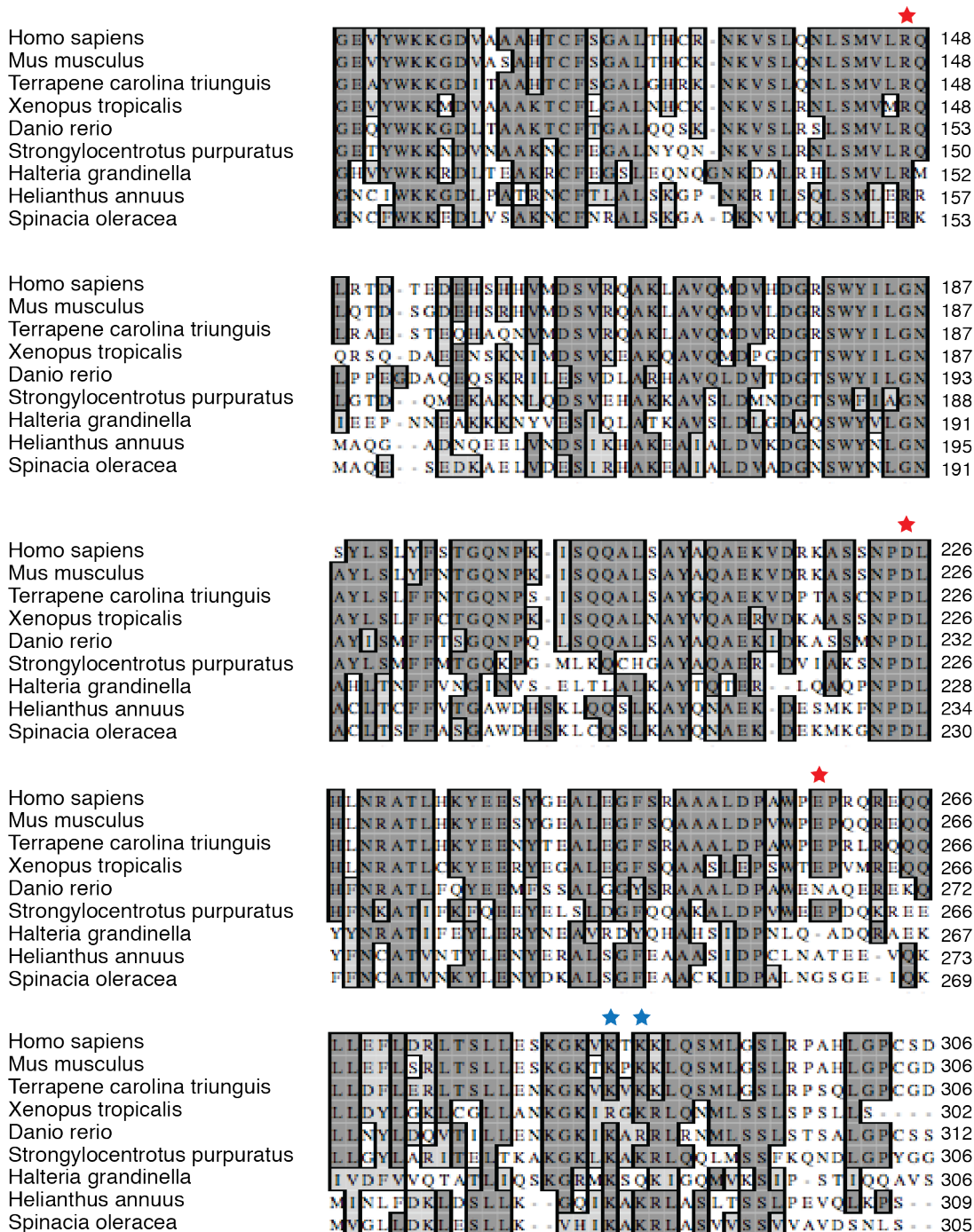


Fig. S2 - Multiple sequence alignment of TTC5 from several species by ClustalW

The residues of human TTC5 that were mutated to disrupt its interaction with tubulin nascent chains or the ribosome are indicated by red and blue asterisks, respectively. The common names of the species that are shown are, in order, human, mouse, turtle, frog, zebrafish, sea urchin, spirotrich ciliate, sunflower, and spinach.

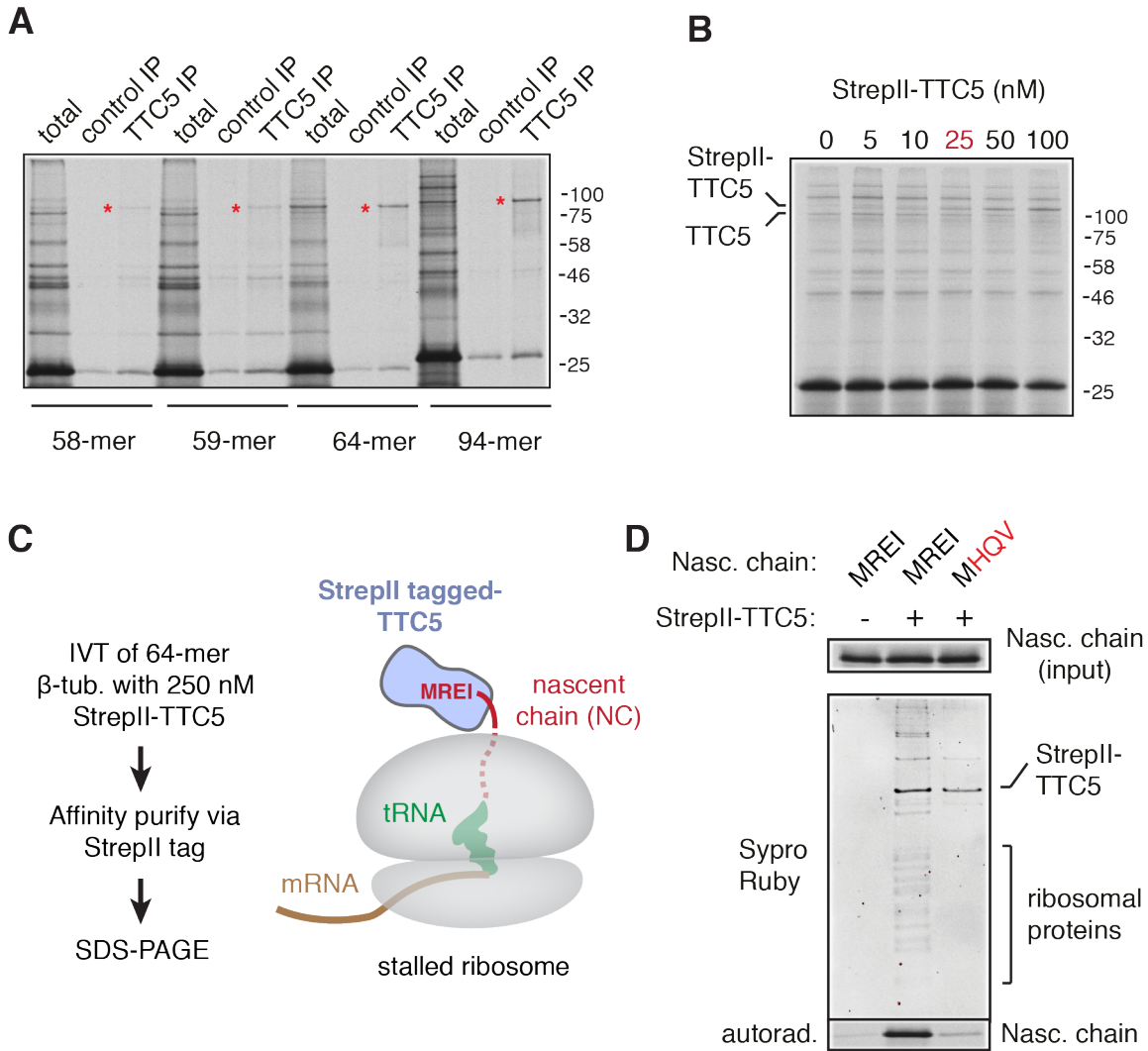


Fig. S3 - Preparation of a ribosome-nascent chain (RNC) complex with TTC5

(A) Analysis of TTC5 crosslinking to different lengths of nascent β -tubulin shows maximal crosslinking at 64 amino acids or longer. Crosslinking analysis was performed as depicted in Fig. 1A. For each length, an aliquot of the total crosslinking reaction is shown together with immunoprecipitation (IP) using control or TTC5 antibodies. Red asterisks indicate the TTC5 crosslink. (B) Titration of recombinant StrepII-tagged TTC5 into the reticulocyte lysate translation reaction and analysis by photo-crosslinking as in Fig. 1B. Endogenous TTC5 is competed by recombinant TTC5, with $\sim 50\%$ competition at 25 nM. (C) Experimental strategy based on the results from panels A and B to assemble and purify the TTC5-RNC complex for cryo-EM analysis. (D) Analysis of TTC5-RNC purifications performed using nascent chains containing wild type or mutant β -tubulin. Ribosomes and the nascent chain are only recovered in the StrepII-based affinity purification when StrepII-TTC5 is included in the reaction. Recovery is lost if the N-terminus of β -tubulin is mutated. Note that crosslinking was not used because the TTC5-RNC complex remained stable during the purification.

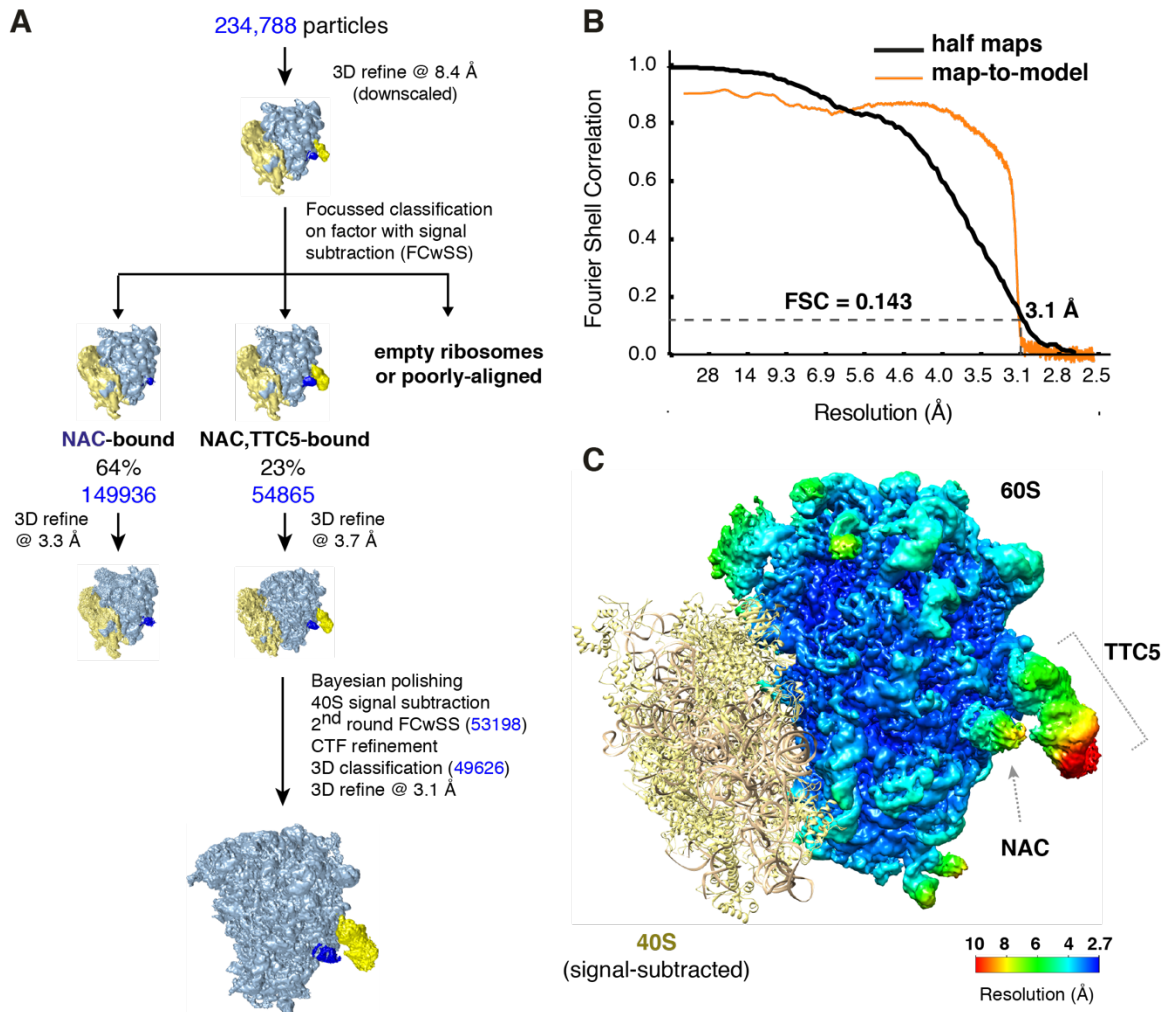


Fig. S4 - Cryo-EM analysis of the TTC5-RNC complex

(A) Classification and reconstruction scheme of ribosomal particles from the EM micrographs. (B). Fourier shell correlation curves for the independent half maps of the 60S-TTC5 reconstruction (black) and between the final map and refined model (orange). (C) Local resolution of the 60S-TTC5 map. The sites of direct interaction between TTC5 and the ribosome were at ~ 3 to 3.5 Å resolution. The remainder of TTC5 varied in resolution, but was sufficient to dock a previous crystal structure of mouse TTC5 and make minor adjustments as necessary (see Fig. S5). The ubiquitous ribosome binding protein NAC was observed in our reconstructions but was not investigated or analyzed further in this study.

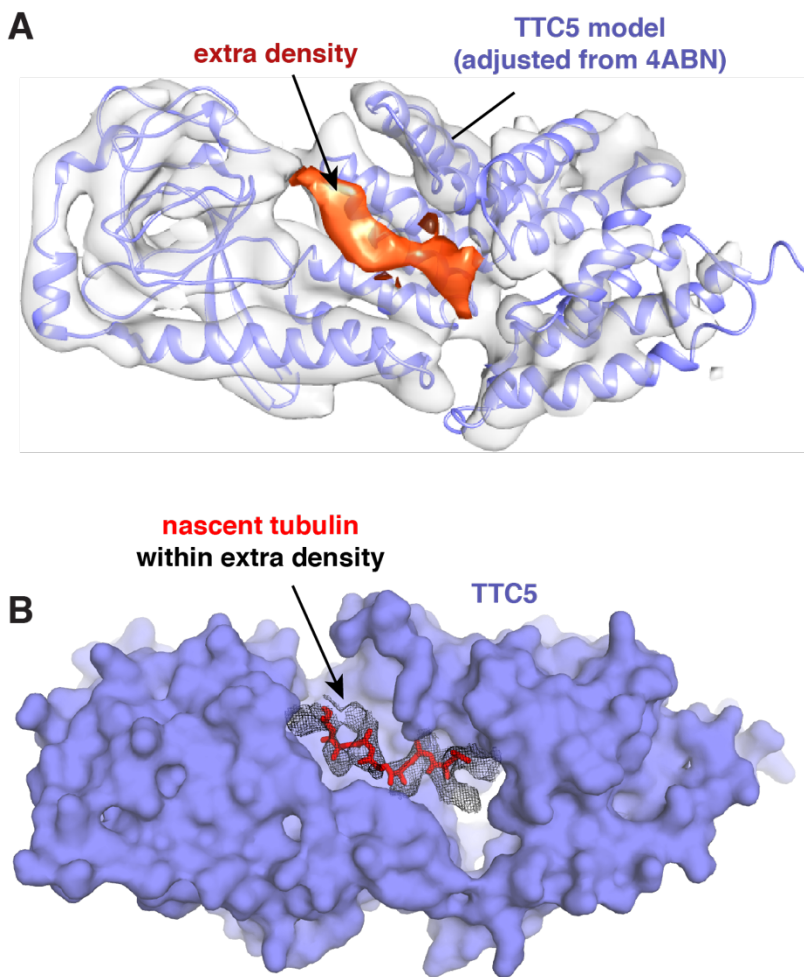


Fig. S5 - Experimental density for nascent tubulin within TTC5

(A) Shown is the unsharpened density map for TTC5 fitted with the human TTC5 homology model adjusted from the crystal structure of mouse TTC5 (4ABN). Additional density (orange) that is not accounted by TTC5 is shown inside the putative binding groove. (B) Space-filling model of TTC5 with the sharpened density within the groove shown in wire mesh. The model for the backbone of β -tubulin with C- β atoms for side chains is shown in red.

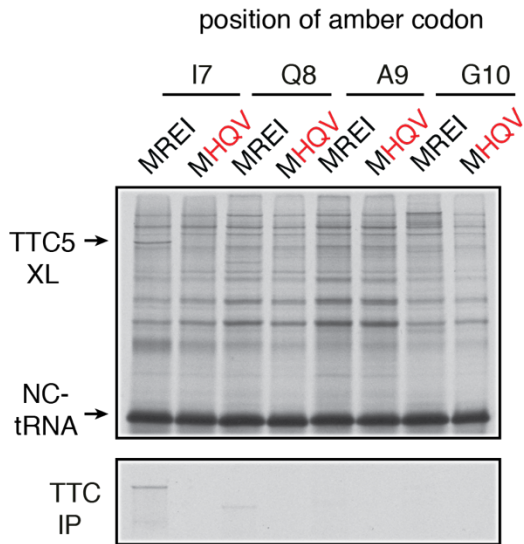


Fig. S6 – Position-dependent crosslinking of TTC5 to nascent β -tubulin

Codon 7, 8, 9 or 10 of β -tubulin was replaced with an amber codon in order to incorporate the UV crosslinking unnatural amino acid Bpa at that position. The crosslinking products were immunoprecipitated by TTC5 antibody. Very poor crosslinking from position 8 and no crosslinking from positions 9 and 10 are seen. This result is consistent with the assignment of β -tubulin within the TTC5 binding groove. Note that crosslinked products often migrate anomalously on SDS-PAGE, as seen for the crosslink to TTC5 from position 7 versus position 8.

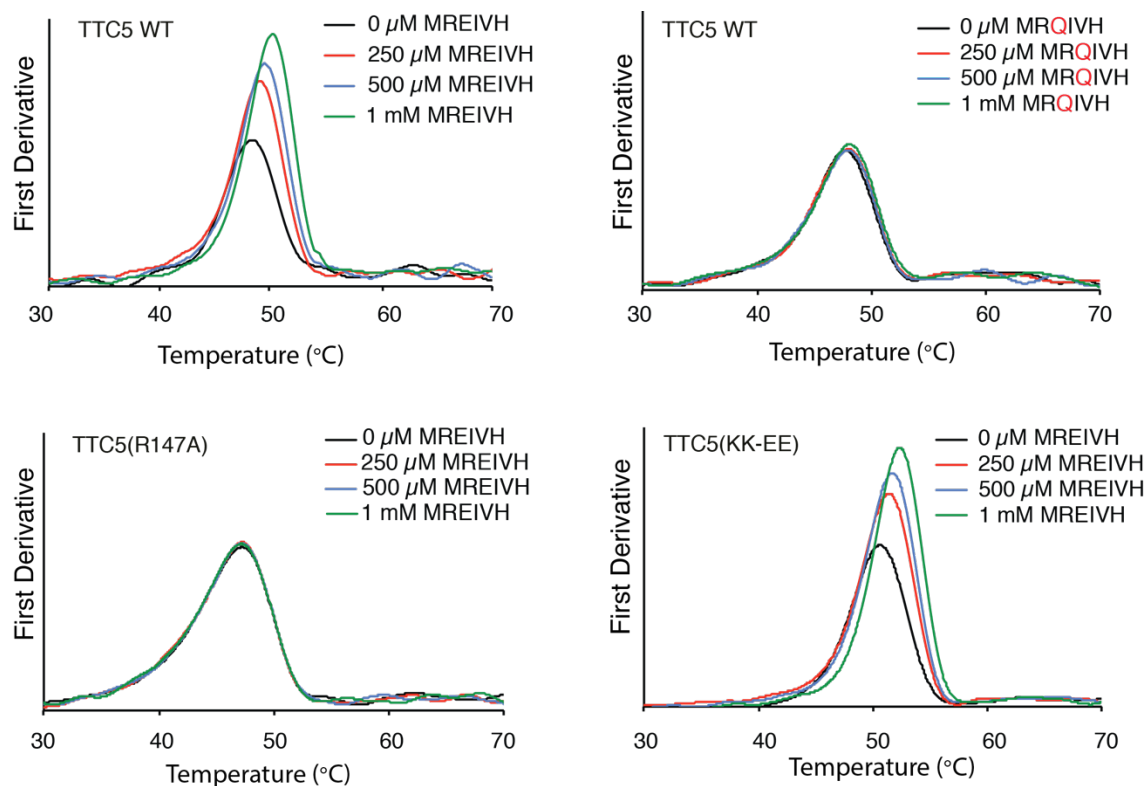


Fig. S7 - Recombinant TTC5 binding to β -tubulin peptides

The binding interaction between recombinant TTC5 and a synthetic peptide of the first six amino acids of β -tubulin was analysed by a thermal shift assay in which denaturation of TTC5 is monitored by intrinsic tryptophan fluorescence. Each plot shows the first derivative of the denaturation curve. The peak represents the inflection point of the sigmoidal denaturation curve. The indicated combinations of recombinant TTC5 and peptide were mixed and subjected to progressive temperature shifts. The denaturation temperature of recombinant wild type TTC5 is shifted by wild type β -tubulin peptide (upper left panel). Exactly the same result was seen for the ribosome binding deficient mutant TTC5 (KK-EE). Mutating either the peptide (upper right) or the binding pocket of TTC5 (i.e., R147A; lower left) completely abolished the interaction. The interactions tabulated in Fig. 3C were determined in exactly the same manner and showed either wild type level of binding or no detectable binding as indicated in the table.

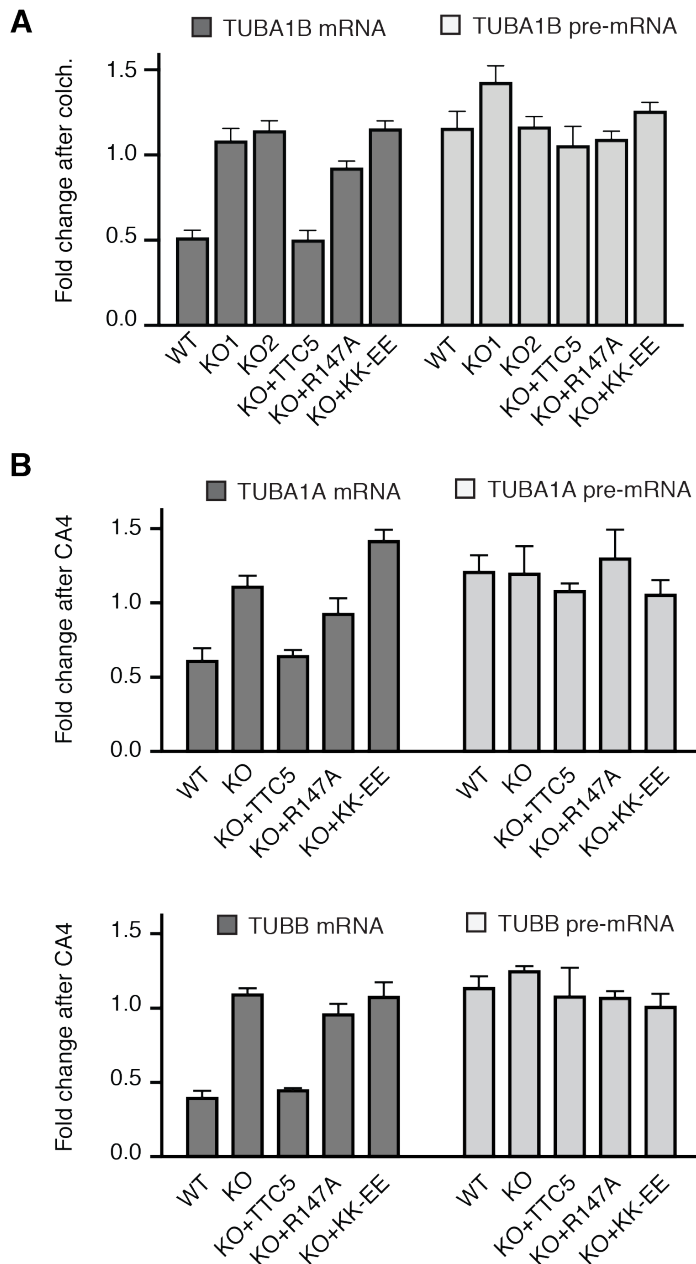


Fig. S8 - Tubulin mRNA degradation requires TTC5 at the ribosome

(A) The indicated HEK293 cell lines were either left untreated or treated for 3 h with colchicine. The relative amounts of the indicated mRNAs or pre-mRNAs were quantified by RT-qPCR and normalized to a control ribosomal RNA. The fold-change after colchicine treatment relative to the untreated sample for each cell line is plotted (mean \pm SEM from three replicates). (B) The indicated HeLa cell lines were either left untreated or treated for 4 h with combretastatin A4 (CA4). The relative amounts of the indicated mRNAs or pre-mRNAs were quantified by RT-qPCR and normalized to a reference gene (GAPDH). The fold-change after CA4 treatment relative to the untreated sample for each cell line is plotted (mean \pm SEM from three replicates).

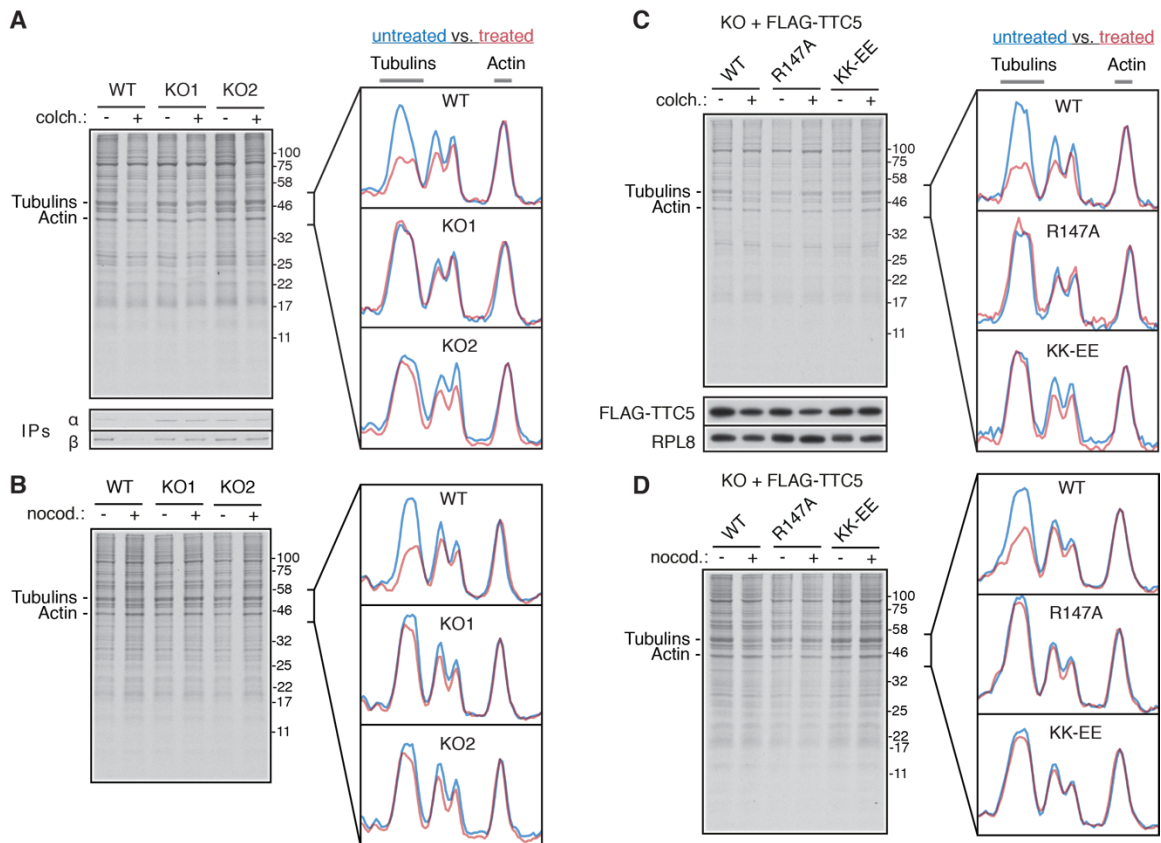


Fig. S9 - TTC5 is required for tubulin autoregulation

(A-D) The indicated HEK293 cell lines were either left untreated or treated for 3 h with colchicine (colch.) or nocodazole (nocod.) before pulse-labelling for 30 min with ³⁵S-methionine. The total products were visualized by autoradiography. The indicated region of the autoradiograph containing tubulins and actin was analyzed by scanning densitometry. The traces, normalized to the actin band, are shown from untreated (blue) and nocodazole-treated (red) samples for each cell line. Autoregulation is only seen in cells containing wild type TTC5.

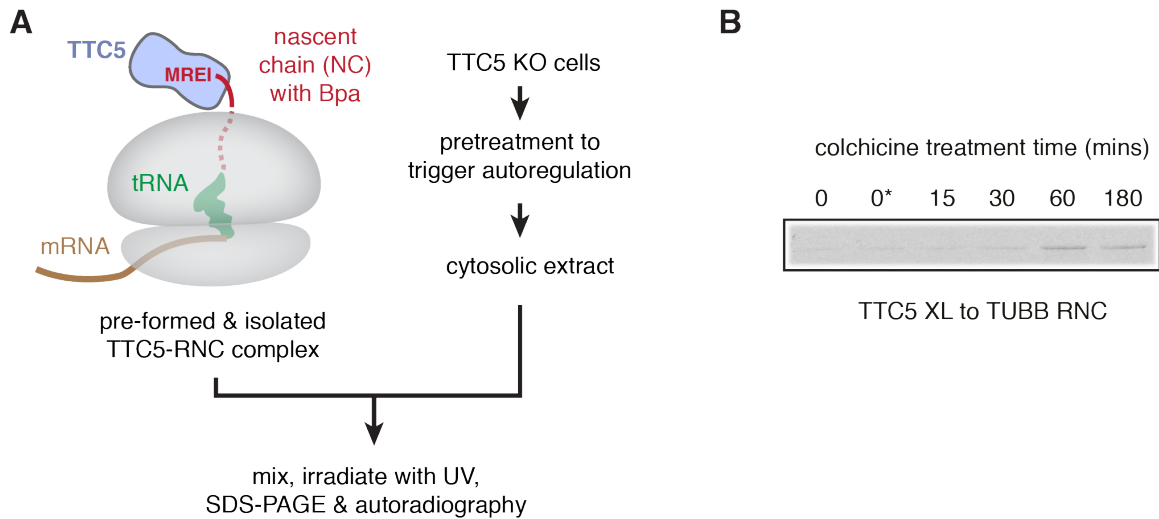


Fig. S10 - Detection of a TTC5 inhibitor that is lost in colchicine-treated cells

(A) Diagram depicting the protocol for the experiments shown in Fig. 4B and fig. S10B. ³⁵S-labelled 94-mer β -tubulin nascent chain containing Bpa at position 7 is prepared in reticulocyte lysate (as in Fig. 1A) and the RNC-TTC5 complex is isolated by centrifugation. This pre-formed RNC-TTC5 complex is then mixed with cytosolic lysate from TTC5 knockout cells that had been pre-treated (+col) or not (-col) with colchicine for up to 3 hours to initiate autoregulation. TTC5 knockout cells were used to ensure that the only TTC5 in the reaction was from the pre-formed TTC5-RNC complex. While autoregulation cannot be executed in these cells due to the absence of TTC5, we reasoned that cells would still trigger the process. The samples are then subjected to UV crosslinking to monitor the nascent chain interactions. (B) An experiment similar to Fig. 4B (and diagrammed in fig. S10A) was performed and the TTC5 crosslinked product was recovered by immunoprecipitation via TTC5. Shown is the autoradiograph visualizing the TTC5-nascent chain crosslinked product. Lysate from untreated cells completely disrupts the TTC5-RNC interaction, so no crosslinked product is seen. When cells are pre-treated with colchicine, the inhibitory activity that disrupts the TTC5-RNC interaction is progressively lost, and the crosslink is observed. This suggests that untreated lysate contains an inhibitor of the TTC5-RNC interaction that is not active or not present in the colchicine-treated lysate. One of the control samples included colchicine added after cell lysis (indicated as 0*). This post-lysis treatment did not inactivate the inhibitor, which is only inactivated over time when the autoregulation signal is initiated in live cells.

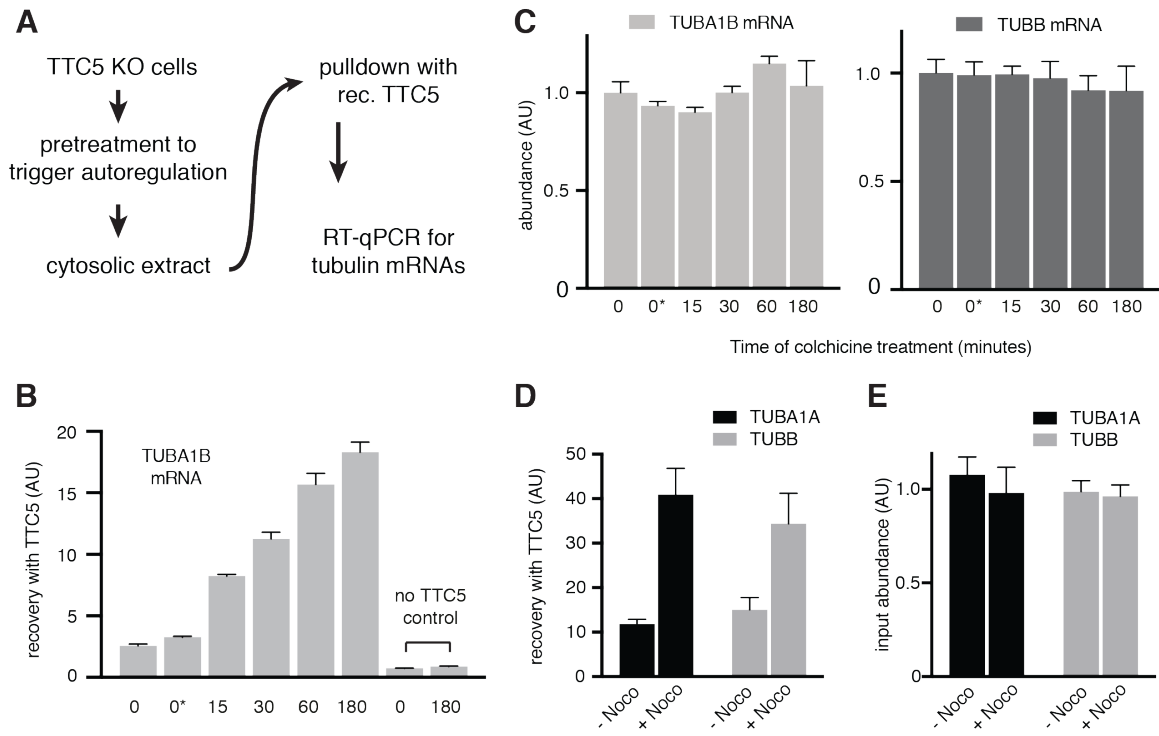


Fig. S11 - TTC5 engages tubulin mRNAs preferentially during autoregulation

(A) Experimental strategy for Fig. 4C and fig. S10B. TTC5 knockout cells were used to ensure that tubulin mRNA content does not change during the experiment (verified in fig. S11C). While autoregulation cannot be executed in these cells due to the absence of TTC5, we reasoned that cells would still trigger the process. (B) TTC5-knockout HEK293 cells were pre-treated for the indicated times with colchicine and used to prepare lysates (as in Fig.4C). One of the control samples included colchicine added after cell lysis (indicated as 0*). Each lysate was incubated with immobilized recombinant TTC5 and the recovered products were analyzed for the indicated α - and β -tubulin mRNAs by quantitative RT-PCR. The relative recoveries of tubulin mRNAs to a ribosomal protein mRNA are plotted (mean \pm SD from three biological replicates). Control pulldowns using resin lacking TTC5 were analyzed in parallel. (C) Aliquots of the same lysates prepared for panel A and Fig. 4C were analyzed for total α - and β -tubulin mRNAs by quantitative RT-PCR. The abundances of tubulin mRNAs relative to a ribosomal protein mRNA are plotted (mean \pm SD from three replicates). As expected for TTC5 knockout cells, neither alpha nor beta tubulin mRNAs change their abundance during this time of colchicine treatment. (D) TTC5-knockout HEK293 cells were left untreated or pre-treated with nocodazole for 15 minutes and used to prepare lysates. Each lysate was incubated with immobilized recombinant TTC5 and the recovered products were analyzed for the indicated α - and β -tubulin mRNAs by quantitative RT-PCR. The relative recoveries of tubulin mRNAs to a ribosomal protein mRNA are plotted (mean \pm SD from three biological replicates). (E) Aliquots of the input lysates prepared in panel D were analyzed for total α - and β -tubulin mRNAs by quantitative RT-PCR. The abundances of tubulin mRNAs relative to a ribosomal protein mRNA are plotted (mean \pm SD from three biological replicates).

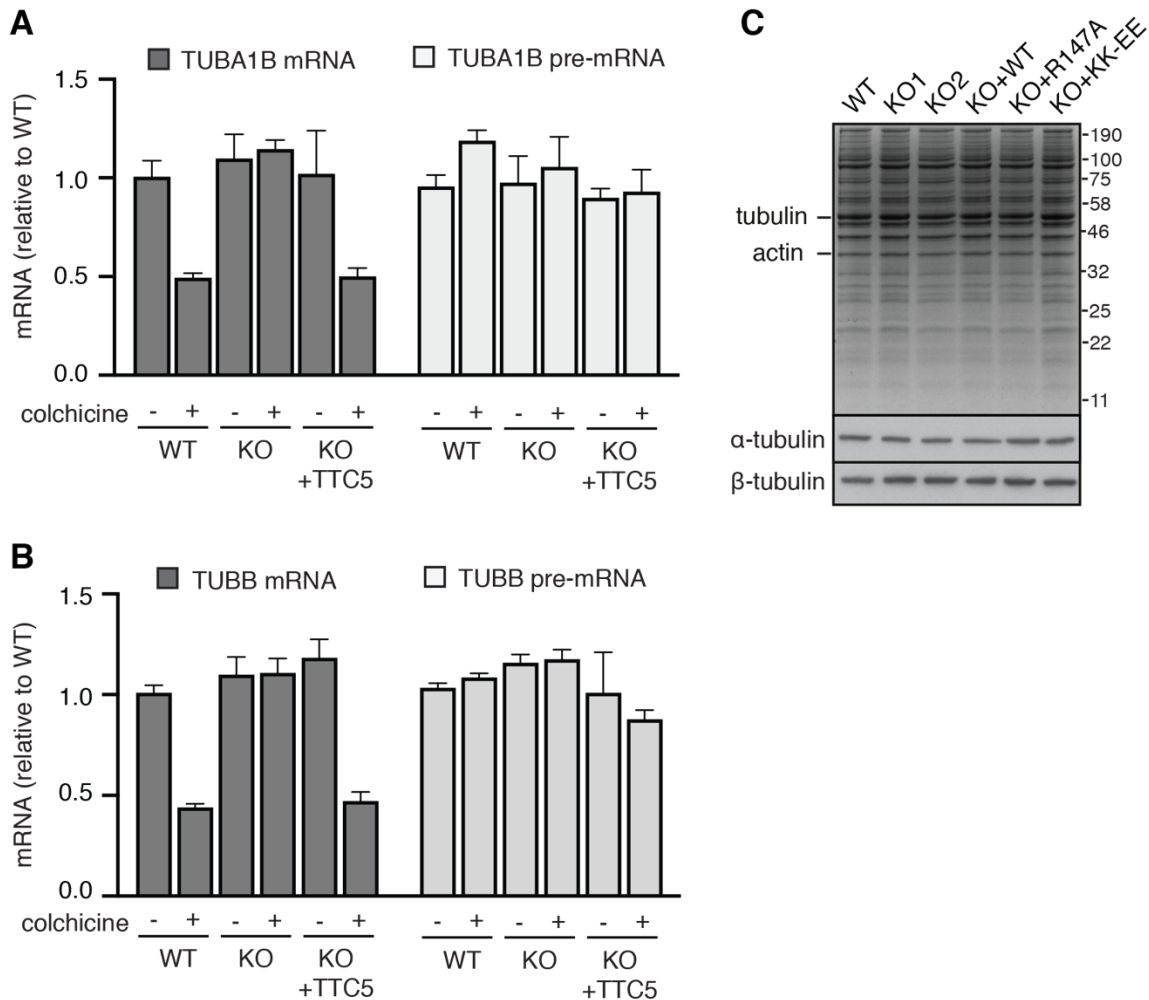


Fig. S12. TTC5 knockout cells have normal tubulin mRNA and protein levels

(A, B) The indicated HEK293 cell lines were either left untreated or treated for 3 h with colchicine. The relative amounts of α -tubulin (panel A) and β -tubulin (panel B) mRNAs or pre-mRNAs were quantified by RT-qPCR and normalized to a control ribosomal RNA. Plotted is the mean \pm SD from three biological replicates. Note that relative to wild type cells (arbitrarily set at 1), the tubulin mRNA levels are not appreciably changed in TTC5 knockout (KO) cells or in KO cells rescued by TTC5 re-expression. As expected, colchicine treatment of WT and KO+TTC5 results in \sim 2-fold reduction in mRNA (but not pre-mRNA). (C) The upper panel shows Coomassie staining of total proteins in lysates from the indicated HEK293 cell lines. An aliquot of the lysates was blotted with the indicated tubulin antibodies (bottom panels). No obvious difference in steady state tubulin levels was observed across the different cell lines. Because these measurements of total tubulin mRNA and protein were on unsynchronized bulk cultures (where the vast majority of cells are not undergoing mitosis at any given moment), subtle differences selectively during mitosis would not be apparent. Future work will be needed to directly measure various aspects of tubulin dynamics either in synchronized cultures or in single cells to determine how the absence of autoregulation perturbs tubulin to impact mitosis.

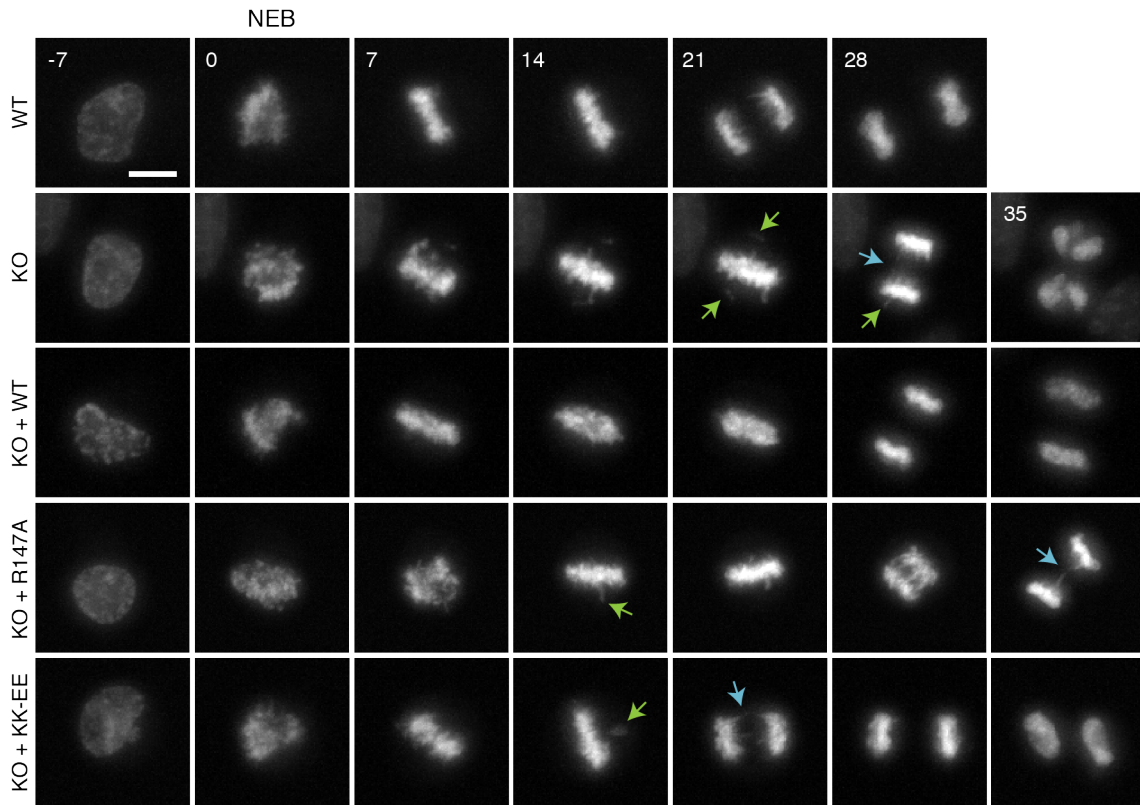


Fig. S13 - Loss of TTC5 compromises mitotic fidelity

Examples of time-lapse images of the indicated HeLa cell lines stained with sirDNA dye. Time (in minutes) relative to nuclear envelope breakdown (NEB) is shown in the upper left of images. Green arrows indicate examples of errors in chromosome alignment onto the metaphase plate. Blue arrows indicate errors in chromosome segregation in anaphase. Scale bar = 5 μ m.

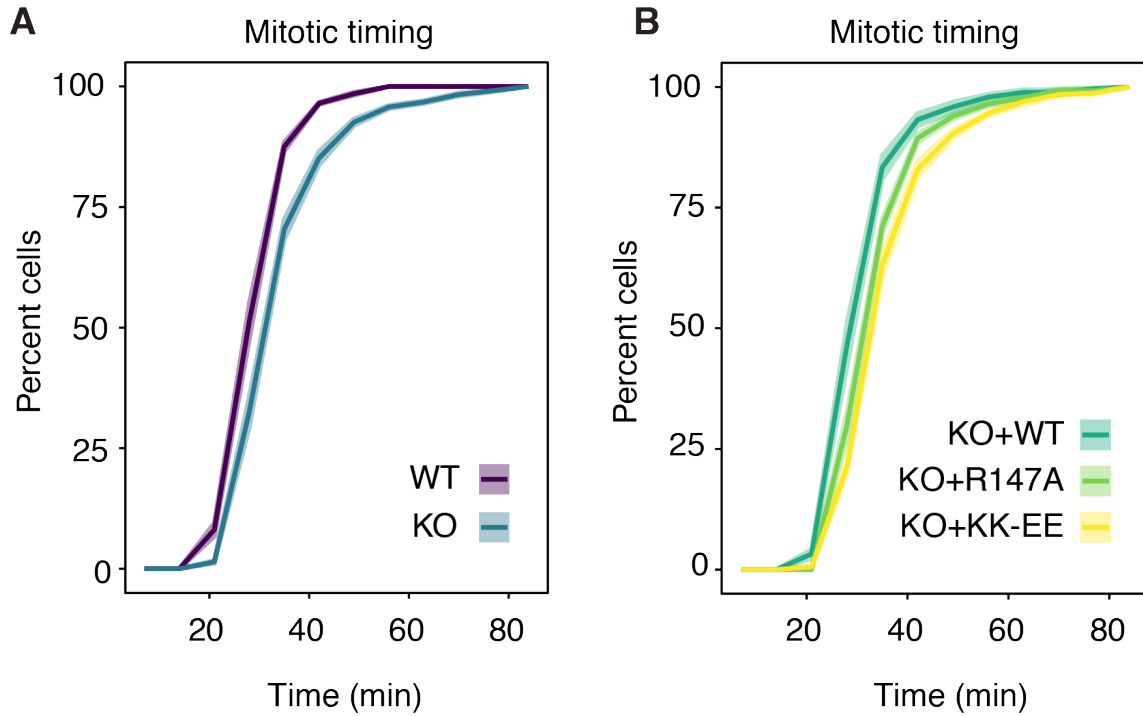


Fig. S14 - Loss of TTC5 delays mitosis

Cumulative frequency of mitotic duration time (from nuclear envelope breakdown to telophase) for the indicated HeLa cell lines. Plotted is the percent of cells that have completed mitosis at each time point. Full lines represent average cumulative frequency, and shaded areas are SEM from 4-6 independent biological replicates and 200-400 analyzed cells.

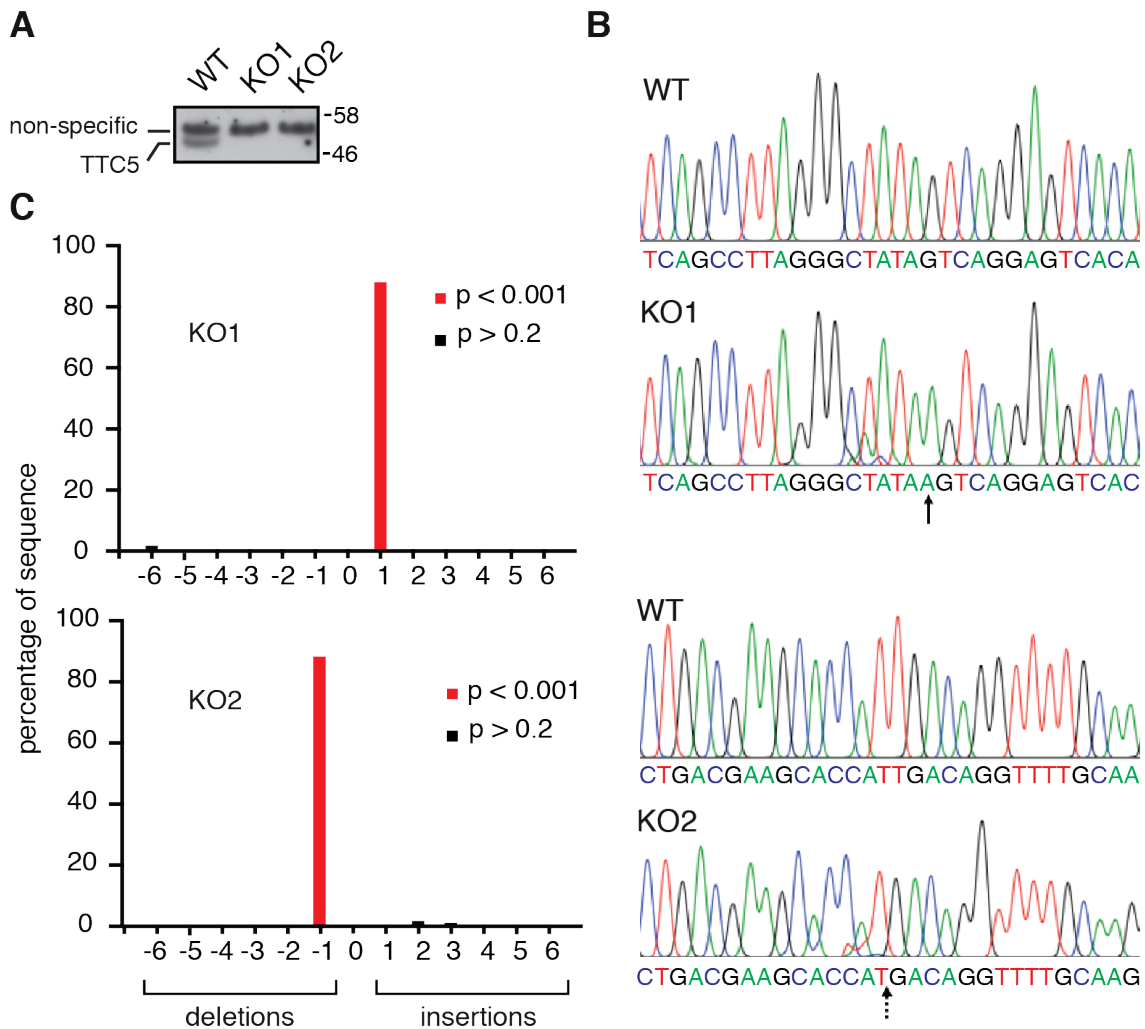


Fig. S15 - Validation of TTC5 knockout cells

(A) Anti-TTC5 western blot analysis of total lysate obtained from WT HEK293 cells or each of two independently derived TTC5-knockout cells generated with different guide RNAs. (B) Genotyping of TTC5-knockout cells. The modified genomic region was amplified via PCR and sequenced. The chromatograms of the amplicons from wild type and TTC5-knockout cells are shown, with arrow indicating the site of a single base insertion (KO1) and single base deletion (KO2). (C) The chromatograms for the knockout cells in panel B were compared to that from WT cells using Tracking of Indels by DEcomposition (TIDE) analysis. The knockout alleles in KO1 are +1 frameshifted and the alleles in KO2 are -1 frameshifted. HeLa cell knockouts were similarly verified.

Table S1.

Data collection, processing, refinement and model statistics.

Data Collection	
Microscope	Titan Krios
Voltage (kV)	300
Magnification (corrected)	104,555
Pixel size (Å)	1.339
Detector	Falcon III
Defocus range (µm)	-0.9 to -2.7
Defocus mean (µm)	-1.8
Total electron exposure (e-Å ⁻²)	48.36
Exposure rate (e-Å ⁻² frame ⁻¹)	1.24
Data collection software	EPU
Data Processing	
Independent data collections	1
Useable micrographs	2669
Particles picked	234788
Final particles	49626
Map sharpening B-factor (Å ²)	-10
Accuracy	
translations (pix) / rotations (°)	0.26 / 0.34°
Resolution (Å)	
Unmasked (0.5 / 0.143 FSC)	3.89 / 3.14
Masked (0.5/0.143 FSC)	3.33 / 2.98
Local resolution range (Å)	13.5-2.7
EMDB accession code	EMD-10380
PDB accession code	6T59
Model Composition	
Chains	53
Non-hydrogen atoms	143,048
Protein residues	7383
RNA bases	3890
Metals (Mg ²⁺ /Zn ²⁺)	220/5
Refinement	
Software	phenix.real_space_refine
Resolution (Å)	3.11
CC (mask)	0.87
CC (main chain)	0.86
CC (side chain)	0.86
Average B factors (Å ²)	
Protein	60.6
Nucleotide	94.1
R.M.S deviations	
Bond lengths (Å)	0.011
Bond angles (°)	0.824
Validation	
Molprobrity score	2.07
Clashscore, all atoms	10.66
Rotamers outliers (%)	0.68
Cβ outliers (%)	0.00
EMRinger score	3.08
CaBLAM outliers (%)	3.24
Ramachandran plot	
Favored (%)	90.92
Allowed (%)	8.98
Outliers (%)	0.10